ELSEVIER

SCIENCE DIRECT®

PHYSICS LETTERS B

Physics Letters B 578 (2004) 109–118

www.elsevier.com/locate/physletb

Sivers function in a spectator model with axial-vector diquarks

Alessandro Bacchetta, Andreas Schäfer, Jian-Jun Yang

Institut für Theoretische Physik, Universität Regensburg, D-93040 Regensburg, Germany

Received 22 September 2003; received in revised form 10 October 2003; accepted 14 October 2003

Editor: P.V. Landshoff

Abstract

We perform a calculation of the Sivers function in a spectator model of the nucleon, with scalar and axial-vector diquarks. We make use of gluon rescattering to produce the nontrivial phases necessary to generate the Sivers function. The inclusion of axial-vector diquarks enables us to obtain a nonzero Sivers function for down quarks. Using the results of our model, we discuss the phenomenology of transverse single spin asymmetries in π^+, π^-, and π^0 production, which are currently analysed by the HERMES and COMPASS Collaborations. We find that the inclusion of axial-vector diquarks substantially reduces the asymmetries.

PACS: 13.60.Le; 13.88.+e; 12.39.Ki

1. Introduction

The Sivers function was introduced for the first time in Ref. [1], in an attempt to explain the observation of single-spin asymmetries in hard hadronic reactions. Since then, some phenomenological extractions of the Sivers function have been performed [2–4], from data on pion production in proton–proton collisions [5,6]. The Sivers function gives a contribution also to the single-spin asymmetry observed by the HERMES Collaboration in pion production via deep inelastic scattering off polarized targets [7–9]. In all the above cases, however, the presence of competing effects (in particular, the Collins effect) did not allow clear conclusions up to now [3,10].

Despite the phenomenological indications, for several years the Sivers function was believed to vanish due to time-reversal invariance [11]. However, this statement was contradicted by an explicit calculation by Brodsky, Hwang and Schmidt, using a spectator model [12]. As the Sivers function is an example of T-odd entity, it requires the interference between two amplitudes with different imaginary parts [11,13]. Spectator models at tree level cannot provide these nontrivial phases, but they can arise as soon as a gluon is exchanged between the struck quark and the target spectator [12]. More generally, the presence of the gauge link, which insures the color gauge invariance of parton distributions, can provide nontrivial phases and thus generate T-odd functions [14–17]. The main ingredient of the model calculation of [12] is nothing else than the one-gluon approximation to the gauge

E-mail addresses: alessandro.bacchetta@physik.uni-regensburg.de (A. Bacchetta), andreas.schaefer@physik.uni-regensburg.de (A. Schäfer), jian-jun.yang@physik.uni-regensburg.de (J.-J. Yang).

doi:10.1016/j.physletb.2003.10.045

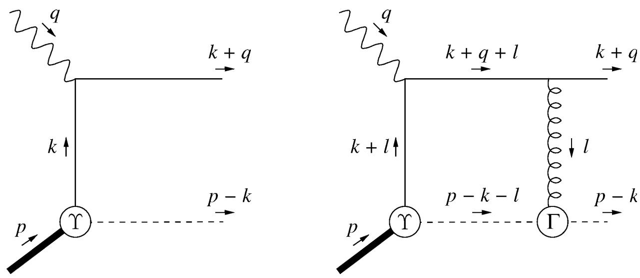

(a) (b)

Fig. 1. Tree-level and one-loop diagrams for the spectator-model calculation of the Sivers function. The dashed line indicates both the scalar and axial-vector diquarks.

link. It is also interesting to note that T-odd distribution functions vanish in a large class of chiral soliton models, where gluonic degrees of freedom are absent [18].

The work of Brodsky, Hwang and Schmidt was not aimed at producing a phenomenological estimate. A step forward in this direction has been accomplished in Refs. [19,20]. In our article, we present an alternative calculation, using the version of the spectator model presented by Jakob, Mulders and Rodrigues in Ref. [21]. In particular, we include in the model a dynamical axial-vector diquark as a possible spectator, and we explore the Sivers function for down quarks. The necessity to include axial-vector diquarks is also discussed, e.g., in Refs. [22–24]. Finally, we point out that a calculation of the Sivers function in the MIT bag model has been recently presented in Ref. [25].

2. Unpolarized distribution function f_1

The unpolarized distribution function f_1 can be defined as

$$f_1\big(x,\vec{k}_T^2\big)=\frac{1}{4}\,\mathrm{Tr}\big[\big(\Phi(x,\vec{k}_T;S)+\Phi(x,\vec{k}_T;-S)\big)\gamma^+\big], \tag{1}$$

where S is the spin of the target. The correlator $\Phi(x,\vec{k}_T)$ can be written as [17]

$$\Phi(x,\vec{k}_T;S)=\int\frac{\mathrm{d}\xi^-\,\mathrm{d}^2\xi_T}{(2\pi)^3}\,\mathrm{e}^{+\mathrm{i}k\cdot\xi}\langle P,S|\bar{\psi}(0)\mathcal{L}_{[0^-,\infty^-]}\mathcal{L}_{[0_T,\infty_T]}\mathcal{L}_{[\infty_T,\xi_T]}\mathcal{L}_{[\infty^-,\xi^-]}\psi(\xi)|P,S\rangle\Big|_{\xi^+=0}, \tag{2}$$

where the notation $\mathcal{L}_{[a,b]}$ indicates a straight gauge link running from a to b. In Drell–Yan processes the link runs in the opposite direction, to $-\infty$ [17]. For the calculation of the unpolarized function f_1 the transverse part of the gauge link does not play a role and the entire gauge link can be reduced to unity. Therefore, for this first part of the calculation it is sufficient to consider only the handbag diagram.

At tree level, we follow almost exactly the spectator model of Jakob, Mulders and Rodrigues [21]. In this model, the proton (with mass M) can couple to a constituent quark of mass m and a diquark. The diquark can be both a scalar particle, with mass M_s, or an axial-vector particle, with mass M_v. The relevant diagram at tree level (identical for the scalar and axial-vector case) is depicted in Fig. 1(a). In our model, the nucleon–quark–diquark vertices are

$$\Upsilon_s=g_s(k^2),\qquad \Upsilon_v^\mu=\frac{g_v(k^2)}{\sqrt{2}}\gamma_5\gamma^\mu. \tag{3}$$

We make use of the dipole form factor

$$g_{s/v}(k^2)=N_{s/v}\frac{(k^2-m^2)(1-x)^2}{(\vec{k}_T^2+L_{s/v}^2)^2}, \tag{4}$$

where

$$\vec{k}_T^2 = -(1-x)k^2 - xM_{s/v}^2 + x(1-x)M^2, \tag{5}$$

$$L_{s/v}^2 = (1-x)\Lambda^2 + xM_{s/v}^2 - x(1-x)M^2. \tag{6}$$

The only difference with respect to Ref. [21] is the form of Υ_v—the vertex involving nucleon, quark, and axial-vector diquark. This change modifies the original results only slightly. Note that our choice of the form factor, defined in Eq. (4), is very different from the Gaussian form factor employed in Ref. [19]. Both choices have the effect of eliminating the logarithmic divergences arising from k_T integration and suppress the influence of the high k_T region, where anyway perturbative corrections should be taken into account [20].

The final results for the unpolarized distribution function f_1 are

$$f_1^s\big(x,\vec{k}_T^2\big) = \frac{g_s^2[(xM+m)^2+\vec{k}_T^2]}{2(2\pi)^3(1-x)(k^2-m^2)^2} = \frac{N_s^2(1-x)^3[(xM+m)^2+\vec{k}_T^2]}{16\pi^3(\vec{k}_T^2+L_s^2)^4}, \tag{7}$$

$$f_1^v\big(x,\vec{k}_T^2\big) = \frac{g_v^2[(xM+m)^2+\vec{k}_T^2+2xmM]}{2(2\pi)^3(1-x)(k^2-m^2)^2} = \frac{N_v^2(1-x)^3[(xM+m)^2+\vec{k}_T^2+2xmM]}{16\pi^3(\vec{k}_T^2+L_v^2)^4}. \tag{8}$$

Both functions can be integrated over the transverse momentum to give

$$f_1^s(x) = \frac{N_s^2(1-x)^3}{96\pi^2 L_s^6}\big[2(xM+m)^2+L_s^2\big], \tag{9}$$

$$f_1^v(x) = \frac{N_v^2(1-x)^3}{96\pi^2 L_v^6}\big[2(xM+m)^2+L_s^2+4xmM\big]. \tag{10}$$

In order to obtain the distribution functions for u and d quarks, we use the following relation, coming from the analysis of the proton wave function

$$f_1^u = \frac{3}{2}f_1^s + \frac{1}{2}f_1^v, \qquad f_1^d = f_1^v. \tag{11}$$

Here we refrain from discussing the choice of parameters of the model and its quality, for which we refer to the original work [21]. We choose the following values for the parameters of the model:

$$m = 0.36\ \text{GeV}, \qquad M_s = 0.6\ \text{GeV}, \qquad M_v = 0.8\ \text{GeV}, \tag{12}$$

$$\Lambda = 0.5\ \text{GeV}, \qquad N_s^2 = 6.525, \qquad N_v^2 = 28.716. \tag{13}$$

The factors N_s and N_v are chosen in order to normalize the functions f_1^s and f_1^v to 1 and consequently to normalize f_1^u to 2 and f_1^d to 1. The results of the model are shown in Fig. 2. The dashed line represents the result of the spectator model with scalar diquarks only (with $f_1^u = 2f_1^s$). As can be seen, the difference for the u distribution is not big, but it is particularly relevant at small x. The d quark distribution is zero when only scalar diquarks are used, which is clearly unrealistic.

One of the problems when trying to match the model and the phenomenology is that it is not clear at which energy scale the model should be applied. A way to estimate this energy scale is to compare the total momentum carried by the valence quarks in the model and in some parametrization [24,26]. Taking, for instance, the CTEQ5L parametrization [27][1] it turns out that this scale is about 0.078 GeV^2. Then, by applying standard DGLAP equations, we can evolve our model results to 1 GeV^2 and compare it with the CTEQ5L parametrization at that scale. The result is shown in Fig. 3. Admittedly, the model reproduces the parametrization of the valence quark distribution only qualitatively. In any case, in this work we mainly aim at giving rough estimates of the relative

[1] We use leading order evolution with three flavors and $\Lambda_{\mathrm{LO}}^{(3)} = 0.222$, in order to match the CTEQ5 results.

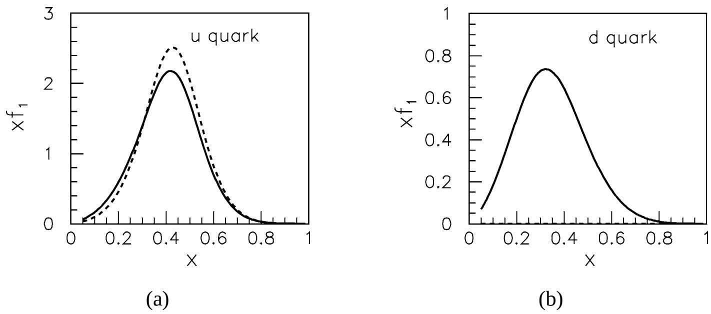

Fig. 2. Model calculation of $xf_1(x)$: with scalar diquarks only (dashed line), with scalar and axial-vector diquarks (solid line). The d quark distribution is zero when only scalar diquarks are used.

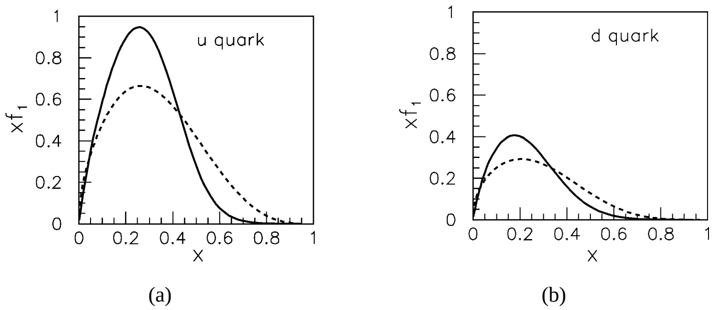

Fig. 3. Model calculation of $xf_1(x)$ (solid line) compared to the CTEQ5L parametrization [27] (dashed line) at 1 GeV^2.

magnitude of the u and d Sivers function and of the related single-spin asymmetries, as well as studying the changes induced in the model results when an axial-vector diquark is introduced. Therefore, we refrain from improving and tuning the model.

3. Sivers function and its moments

We use the following definition of the Sivers function

$$\frac{\epsilon_T^{ij} k_{Ti} S_{Tj}}{M} f_{1T}^{\perp}\big(x, \vec{k}_T^2\big) = -\frac{1}{4} \mathrm{Tr}\big[\big(\Phi(x, \vec{k}_T; S) - \Phi(x, \vec{k}_T; -S)\big)\gamma^+\big], \tag{14}$$

where $4\mathrm{i}\epsilon_T^{ij} k_{Ti} S_{Tj} = \mathrm{Tr}[\gamma_5 \gamma^+ \gamma^- \not{k} \not{S}]$. At tree level the Sivers function turns out to vanish. This is due to the lack of any final state interaction that can provide the imaginary parts necessary to generate T-odd functions. We need to introduce the one-loop amplitude described in Fig. 1(b). This is nothing else than the one-gluon approximation to the gauge link included in Eq. (2). The Sivers function receives a contribution from the interference between amplitude (a) and the imaginary part of amplitude (b). The imaginary part of amplitude (b) can be computed by applying Cutkosky rules or, equivalently, by taking the imaginary part of the propagator $1/(l^+ + \mathrm{i}\epsilon)$ [15]. Note that in Drell–Yan processes the different topology of the one-gluon diagram implies that the imaginary part of the propagator $1/(l^+ - \mathrm{i}\epsilon)$ has to be taken, with the effect of changing the overall sign of the Sivers function [14,28]. This is consistent with the change in direction of the gauge link mentioned before [17].

Following Ref. [12] we perform the calculations initially with Abelian gluons and generalize the result to QCD at the end. We use Feynman gauge. In order to compute the one-loop diagram, we have to make the appropriate choice for the vertex between the gluon and the scalar or axial-vector diquark. We choose the following forms

$$\Gamma_s^{\mu} = -\mathrm{i}e_2(2p-2k-l)^{\mu}, \tag{15}$$

$$\Gamma_v^{\mu,\alpha\beta} = \mathrm{i}e_2\big[(2p-2k-l)^{\nu} g^{\alpha\beta} - (p-k-vl)^{\beta} g^{\nu\alpha} - \big(p-k-(1-v)l\big)^{\alpha} g^{\nu\beta}\big], \tag{16}$$

where e_2 denotes the color charge of the diquark, which we assume to be the same for both kinds of diquark. The gluon–axial-vector diquark coupling is identical to the photon–axial-vector diquark coupling suggested in Ref. [22]. The parameter v is the anomalous magnetic moment of the axial-vector diquark; for $v=1$ the vertex is analogous, for instance, to the standard photon–W vertex. In any case, our results at leading order do not depend on the anomalous magnetic moment of the diquark.

The final results for the Sivers function are

$$f_{1T}^{\perp s}\big(x,\vec{k}_T^2\big) = \frac{e_1 e_2 N_s^2 (1-x)^3 M(xM+m)}{4(2\pi)^4 L_s^2\big[\vec{k}_T^2 + L_s^2\big]^3}, \tag{17}$$

$$f_{1T}^{\perp v}\big(x,\vec{k}_T^2\big) = -\frac{e_1 e_2 N_v^2 (1-x)^3 x M^2}{8(2\pi)^4 L_v^2\big[\vec{k}_T^2 + L_v^2\big]^3}. \tag{18}$$

Note that our result for the scalar diquark has the opposite sign compared to similar computations [12,20]. However, a sign error in those computations has been recently identified [29]. The other differences between our results and those in Refs. [12,19,20] are due to the different choice of form factors in the nucleon–quark–diquark vertex. Unfortunately, we cannot evolve our results to a higher energy scale, as we have done for the unpolarized distribution function, since the evolution equations for the Sivers function have not been established yet [30,31]. We hope, however, that the Q^2 dependence of our results is not very strong.

We introduce the k_T moments

$$f_{1T}^{\perp(1/2)}(x) \equiv \int \mathrm{d}^2\vec{k}_T\, \frac{|\vec{k}_T|}{2M} f_{1T}^{\perp}\big(x,\vec{k}_T^2\big), \qquad f_{1T}^{\perp(1)}(x) \equiv \int \mathrm{d}^2\vec{k}_T\, \frac{\vec{k}_T^2}{2M^2} f_{1T}^{\perp}\big(x,\vec{k}_T^2\big), \tag{19}$$

for which we get the following results:

$$f_{1T}^{\perp(1/2)s}(x) = \frac{e_1 e_2 N_s^2 (1-x)^3 (xM+m)}{1024\pi^2 L_s^5}, \qquad f_{1T}^{\perp(1)s}(x) = \frac{e_1 e_2 N_s^2 (1-x)^3 (xM+m)}{256\pi^3 M L_s^4}, \tag{20}$$

$$f_{1T}^{\perp(1/2)v}(x) = -\frac{e_1 e_2 N_v^2 (1-x)^3 xM}{2048\pi^2 L_v^5}, \qquad f_{1T}^{\perp(1)v}(x) = -\frac{e_1 e_2 N_v^2 (1-x)^3 x}{512\pi^3 L_v^4}. \tag{21}$$

The only parameter to be fixed is the product of the quark and diquark charges. Following Ref. [12] we fix $e_1 e_2 = 4\pi C_F \alpha_s$ and we choose $C_F = 4/3$ and $\alpha_S \approx 0.3$.

Relations equivalent to those of Eq. (11) hold for the Sivers function and its moments. In Fig. 4 we show the model results for the first moment of the Sivers function. The inclusion of the axial-vector diquark results in some change to the u Sivers function and allows us to produce a nonzero d quark Sivers function. It turns out in particular that the d Sivers function is much smaller than the u one and has the opposite sign. This result is in qualitative agreement with the bag-model calculation of Ref. [25]. The opposite sign of the two functions is also in agreement with the only phenomenological extractions available at present [2,3,32]. However, there is a sharp difference in the relative magnitude of the two contributions, since in the phenomenological extractions the absolute value of the d contribution is about half of the u contribution, while in our model calculation the d contribution is only about $1/10$ of the u contribution. We point out that this difference could be due to a sizeable contribution of sea quarks (in particular, $\bar{u}$) to the asymmetry studied in Refs. [2,3].

Note that our model calculation complies with the positivity bound [33]

$$f_{1T}^{\perp(1/2)}(x) \leqslant \frac{1}{2} f_1(x). \tag{22}$$

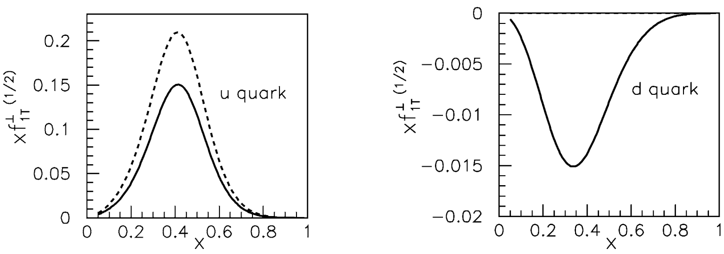

(a) (b)

Fig. 4. Model calculation of $xf_{1T}^{\perp(1/2)}(x)$: with scalar diquarks only (dashed line), with scalar and axial-vector diquarks (solid line). The d quark distribution is zero when only scalar diquarks are used.

We performed also the calculation of the function $h_1^{\perp}$, introduced by Boer and Mulders in Ref. [34] and defined as

$$\frac{\epsilon_T^{ij} k_{Tj}}{M} h_1^{\perp}\big(x, \vec{k}_T^2\big) = \frac{1}{4}\,\mathrm{Tr}\big[\big(\Phi(x, \vec{k}_T; S) + \Phi(x, \vec{k}_T; -S)\big)\mathrm{i}\sigma^{i+}\gamma_5\big]. \tag{23}$$

For the scalar diquark, we found that $h_1^{\perp s} = f_{1T}^{\perp s}$, confirming the results already obtained in Refs. [19,20]. For the axial-vector diquark, we obtain

$$h_1^{\perp v}\big(x, \vec{k}_T^2\big) = -\frac{e_1 e_2 N_v^2 (1-x)^3 M(2xM+m)}{4(2\pi)^4 L_v^2 \big[\vec{k}_T^2 + L_v^2\big]^3}, \qquad h_1^{\perp(1)v}(x) = -\frac{e_1 e_2 N_v^2 (1-x)^3 (2xM+m)}{256\pi^3 M L_v^4}. \tag{24}$$

4. Single spin asymmetries

We consider the weighted transverse spin asymmetries

$$\big\langle \sin(\phi_h - \phi_S)\big\rangle_{\mathrm{UT}}(x,z) = \frac{\int \mathrm{d}y\, \mathrm{d}\phi_S\, \mathrm{d}^2\vec{P}_{h\perp}\, \sin(\phi_h - \phi_S)(\mathrm{d}^6\sigma_{U\uparrow} - \mathrm{d}^6\sigma_{U\downarrow})}{\int \mathrm{d}y\, \mathrm{d}\phi_S\, \mathrm{d}^2\vec{P}_{h\perp}\, (\mathrm{d}^6\sigma_{U\uparrow} + \mathrm{d}^6\sigma_{U\downarrow})}, \tag{25}$$

$$\left\langle \frac{|\vec{P}_{h\perp}|}{zM} \sin(\phi_h - \phi_S)\right\rangle_{\mathrm{UT}}(x,z) = \frac{\int \mathrm{d}y\, \mathrm{d}\phi_S\, \mathrm{d}^2\vec{P}_{h\perp}\, [|\vec{P}_{h\perp}|/(zM)] \sin(\phi_h - \phi_S)(\mathrm{d}^6\sigma_{U\uparrow} - \mathrm{d}^6\sigma_{U\downarrow})}{\int \mathrm{d}y\, \mathrm{d}\phi_S\, \mathrm{d}^2\vec{P}_{h\perp}\, (\mathrm{d}^6\sigma_{U\uparrow} + \mathrm{d}^6\sigma_{U\downarrow})}, \tag{26}$$

where the notation $\mathrm{d}\sigma_{U\uparrow}$ indicates the cross section with an unpolarized lepton beam off a transversely polarized target. The angles involved in the definition of the asymmetry are depicted in Fig. 5. These asymmetries are currently measured by the HERMES and COMPASS Collaborations [35,36].

Under the assumption that the pion transverse momentum with respect to the virtual photon is entirely due to the intrinsic transverse momentum of partons, i.e., $\vec{P}_{h\perp} = z\vec{k}_T$, the first asymmetry can be written as

$$\big\langle \sin(\phi_h - \phi_S)\big\rangle_{\mathrm{UT}}(x,z) \approx \frac{(1/x)\sum_a e_a^2 f_{1T}^{\perp(1/2)a}(x) D_1^a(z)}{(1/x)\sum_a e_a^2 f_1^a(x) D_1^a(z)}, \tag{27}$$

with a indicating the quark flavor. Our model results are displayed in Fig. 6. We took the unpolarized fragmentation functions from Ref. [37] at a scale $Q^2 = 1\ \mathrm{GeV}^2$. In order to make predictions useful for the HERMES experiment, to produce Fig. 6(a) and (b) we integrated the asymmetries over z from 0.2 to 0.7. To produce Fig. 6(c) and (d) we integrated the asymmetries over x from 0.023 to 0.4.

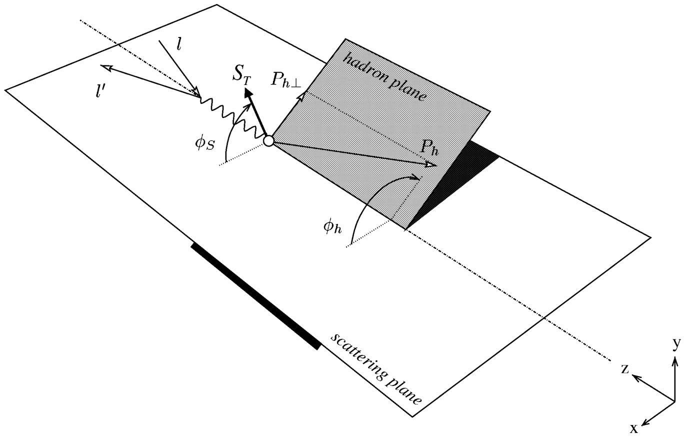

Fig. 5. Description of the vectors and angles involved in the Sivers asymmetry measurement.

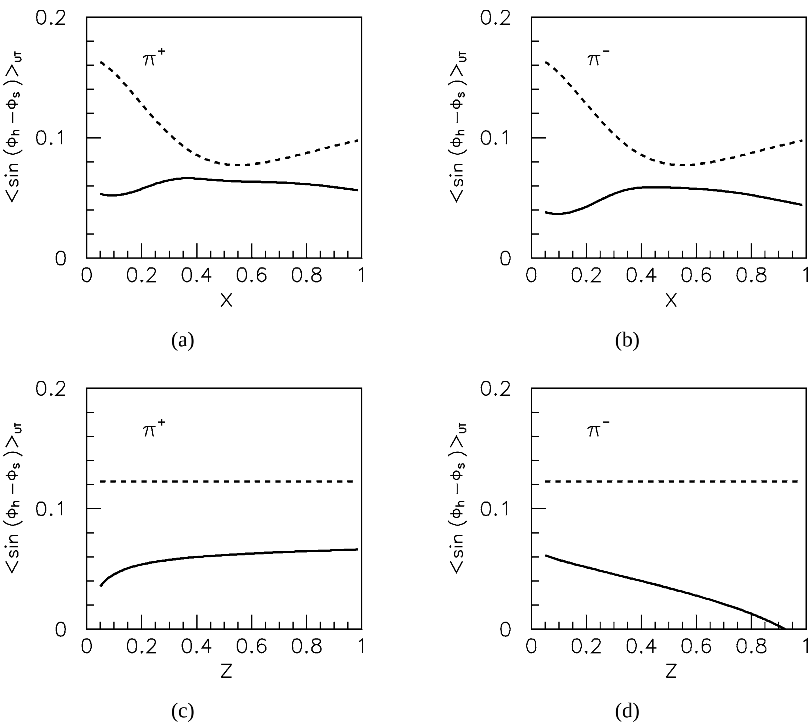

Fig. 6. Model estimate of the single-spin asymmetry $\langle\sin(\phi_h - \phi_S)\rangle_{\mathrm{UT}}$: with scalar diquarks only (dashed line), with scalar and axial-vector diquarks (solid line). The x and z dependence is shown for π^+ and π^-.

Evidently, there is not a big difference between π^+ and π^- asymmetries. We do not plot the results for π^0 production, since they lie between the previous two. We point out that assuming

$$f_1^d D_1^{d(\pi^{\pm,0})} \ll 4 f_1^u D_1^{u(\pi^{\pm,0})}, \tag{28}$$

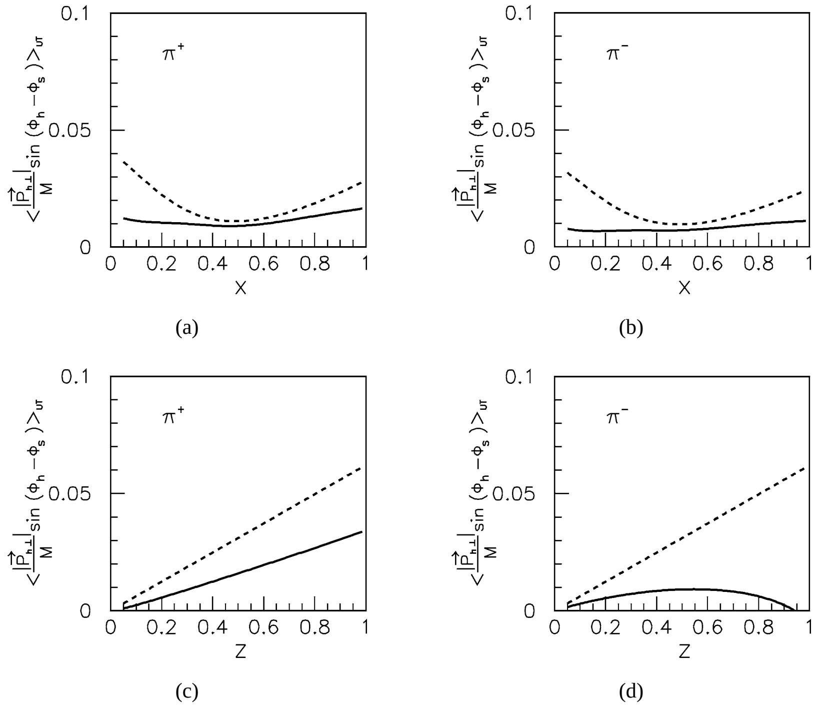

Fig. 7. Model estimate of the single-spin asymmetry $\langle \frac{|P_{h\perp}|}{M} \sin(\phi_h - \phi_S) \rangle_{\mathrm{UT}}$: with scalar diquarks only (dashed line), with scalar and axial-vector diquarks (solid line). The x and z dependence is shown for π^+ and π^-.

the above asymmetry can be written as

$$\langle \sin(\phi_h - \phi_S) \rangle_{\mathrm{UT}}^{\pi^{\pm,0}}(x, z) \approx \frac{3}{2} \frac{f_{1T}^{\perp(1/2)s}(x)}{f_1^u(x)} + \frac{1}{2} \frac{f_{1T}^{\perp(1/2)v}(x)}{f_1^u(x)} \left(1 + \frac{1}{2} \frac{D_1^{d(\pi^{\pm,0})}(z)}{D_1^{u(\pi^{\pm,0})}(z)}\right). \tag{29}$$

The first term in this equation is the dominant one. This explains why there are only small differences between the π^+ and π^- asymmetry. However, the axial-vector contribution to f_1^u cannot be neglected. From Eq. (29) it is also evident that the dependence of the asymmetries on z is due to the influence of the unfavoured fragmentation functions. In the case of π^- the last term in Eq. (29) is bigger and therefore the z dependence is stronger. In the case of π^0—not shown in our pictures—the term in parentheses would be exactly $3/2$ and the z-dependent asymmetry would be a flat line at about 5%.

The asymmetry in Eq. (26) can be written in an assumption-free way as

$$\left\langle \frac{|\vec{P}_{h\perp}|}{M} \sin(\phi_h - \phi_S) \right\rangle_{\mathrm{UT}}(x, z) = \frac{(1/x) \sum_a e_a^2 f_{1T}^{\perp(1)a}(x) z D_1^a(z)}{(1/x) \sum_a e_a^2 f_1^a(x) D_1^a(z)}. \tag{30}$$

The calculated asymmetries are shown in Fig. 7, where we performed the integrations over x or z as in the previous case. As before, assuming Eq. (28) the asymmetry can be simplified to

$$\left\langle \frac{|\vec{P}_{h\perp}|}{M} \sin(\phi_h - \phi_S) \right\rangle_{\mathrm{UT}}^{\pi^{\pm,0}}(x, z) \approx \frac{3}{2} z \frac{f_{1T}^{\perp(1)s}(x)}{f_1^u(x)} + \frac{1}{2} z \frac{f_{1T}^{\perp(1)v}(x)}{f_1^u(x)} \left(1 + \frac{1}{2} \frac{D_1^{d(\pi^{\pm,0})}(z)}{D_1^{u(\pi^{\pm,0})}(z)}\right). \tag{31}$$

5. Conclusions

We calculated the Sivers function in a spectator model of the nucleon with scalar and axial-vector diquarks. The final state interaction necessary to generate T-odd distribution functions was provided by gluon rescattering between the struck quark and the diquark.

The inclusion of axial-vector diquarks allowed us to calculate the Sivers function for the d quarks. The function turns out to have the opposite sign compared to the u quarks and to be much smaller in size. The u quark Sivers function is substantially reduced by the axial-vector contribution. Although the reliability of the model is very limited, we think that our results on the relative behavior of u and d quarks could be qualitatively relevant.

Using the results of our model, we estimated some single spin asymmetries containing the Sivers function. These asymmetries are at present being measured by the HERMES and COMPASS Collaborations. We noticed that the inclusion of axial-vector diquarks can make drastic changes in the asymmetries as compared to the spectator model with scalar diquarks only, particularly at low x. We were able for the first time to estimate the Sivers single spin asymmetry in π^- and π^0 production. We observed that the π^+ and π^- asymmetries are not very different, due to the dominance of the u quark contribution in both cases. The π^0 asymmetries (which we did not show) lie between the π^+ and π^- estimates.

The present approach does not take into account sea quarks. Unfortunately, at the moment we have no indication about the size and sign of the sea-quark Sivers function.

Acknowledgements

Discussion with A. Metz, D.S. Hwang and M. Oettel, M. Stratmann are gratefully acknowledged. The work of A.B. has been supported by the TMR network HPRN-CT-2000-00130 and the BMBF, the work of J.Y. by the Alexander von Humboldt Foundation and by the Foundation for University Key Teacher of the Ministry of Education (China).

References

[1] D.W. Sivers, Phys. Rev. D 41 (1990) 83.
[2] M. Anselmino, F. Murgia, Phys. Lett. B 442 (1998) 470, hep-ph/9808426.
[3] M. Anselmino, M. Boglione, F. Murgia, Phys. Rev. D 60 (1999) 054027, hep-ph/9901442.
[4] M. Anselmino, U. D'Alesio, F. Murgia, Phys. Rev. D 67 (2003) 074010, hep-ph/0210371.
[5] D.L. Adams, et al., FNAL-E704 Collaboration, Phys. Lett. B 264 (1991) 462.
[6] A. Bravar, et al., Fermilab E704 Collaboration, Phys. Rev. Lett. 77 (1996) 2626.
[7] A. Airapetian, et al., HERMES Collaboration, Phys. Rev. Lett. 84 (2000) 4047, hep-ex/9910062.
[8] A. Airapetian, et al., HERMES Collaboration, Phys. Rev. D 64 (2001) 097101, hep-ex/0104005.
[9] A. Airapetian, et al., HERMES Collaboration, Phys. Lett. B 562 (2003) 182, hep-ex/0212039.
[10] A.V. Efremov, K. Goeke, P. Schweitzer, Phys. Lett. B 568 (2003) 63, hep-ph/0303062.
[11] J.C. Collins, Nucl. Phys. B 396 (1993) 161, hep-ph/9208213.
[12] S.J. Brodsky, D.S. Hwang, I. Schmidt, Phys. Lett. B 530 (2002) 99, hep-ph/0201296.
[13] A. Bacchetta, R. Kundu, A. Metz, P.J. Mulders, Phys. Lett. B 506 (2001) 155, hep-ph/0102278.
[14] J.C. Collins, Phys. Lett. B 536 (2002) 43, hep-ph/0204004.
[15] X. Ji, F. Yuan, Phys. Lett. B 543 (2002) 66, hep-ph/0206057.
[16] A.V. Belitsky, X. Ji, F. Yuan, Nucl. Phys. B 656 (2003) 165, hep-ph/0208038.
[17] D. Boer, P.J. Mulders, F. Pijlman, Nucl. Phys. B 667 (2003) 201, hep-ph/0303034.
[18] P.V. Pobylitsa, hep-ph/0212027.
[19] L.P. Gamberg, G.R. Goldstein, K.A. Oganessyan, Phys. Rev. D 67 (2003) 071504, hep-ph/0301018.
[20] D. Boer, S.J. Brodsky, D.S. Hwang, Phys. Rev. D 67 (2003) 054003, hep-ph/0211110.
[21] R. Jakob, P.J. Mulders, J. Rodrigues, Nucl. Phys. A 626 (1997) 937, hep-ph/9704335.

[22] M. Oettel, R. Alkofer, L. von Smekal, Eur. Phys. J. A 8 (2000) 553, nucl-th/0006082.
[23] F.E. Close, A.W. Thomas, Phys. Lett. B 212 (1988) 227.
[24] H. Meyer, P.J. Mulders, Nucl. Phys. A 528 (1991) 589.
[25] F. Yuan, hep-ph/0308157.
[26] A. Bacchetta, S. Boffi, R. Jakob, Eur. Phys. J. A 9 (2000) 131, hep-ph/0003243.
[27] H.L. Lai, et al., CTEQ Collaboration, Eur. Phys. J. C 12 (2000) 375, hep-ph/9903282.
[28] S.J. Brodsky, D.S. Hwang, I. Schmidt, Nucl. Phys. B 642 (2002) 344, hep-ph/0206259.
[29] M. Burkardt, D.S. Hwang, hep-ph/0309072.
[30] A.A. Henneman, D. Boer, P.J. Mulders, Nucl. Phys. B 620 (2002) 331, hep-ph/0104271.
[31] R. Kundu, A. Metz, Phys. Rev. D 65 (2002) 014009, hep-ph/0107073.
[32] M. Boglione, P.J. Mulders, Phys. Rev. D 60 (1999) 054007, hep-ph/9903354.
[33] A. Bacchetta, M. Boglione, A. Henneman, P.J. Mulders, Phys. Rev. Lett. 85 (2000) 712, hep-ph/9912490.
[34] D. Boer, P.J. Mulders, Phys. Rev. D 57 (1998) 5780, hep-ph/9711485.
[35] G. Schnell, HERMES Collaboration, Talk delivered at the 11th International Workshop on Deep Inelastic Scattering (DIS 2003), St. Petersburg, 23–27 April 2003.
[36] P. Pagano, COMPASS Collaboration, Talk delivered at the 11th International Workshop on Deep Inelastic Scattering (DIS 2003), St. Petersburg, 23–27 April 2003.
[37] S. Kretzer, E. Leader, E. Christova, Eur. Phys. J. C 22 (2001) 269, hep-ph/0108055.